Torque ripple reduction of brushless DC motor based on adaptive input-output feedback linearization

M. Shirvani Boroujeni [a], G.R. Arab Markadeh [b,*], J. Soltani [c]

[a] Shahrekord University, Iran
[b] Shahrekord University, Eng. Dept. and Center of Excellence for Mathematics, Shahrekord, Iran
[c] Islamic Azad University, Khomeini shahr Branch, Isfahan, Iran

A B S T R A C T

Torque ripple reduction of Brushless DC Motors (BLDCs) is an interesting subject in variable speed AC drives. In this paper at first, a mathematical expression for torque ripple harmonics is obtained. Then for a non-ideal BLDC motor with known harmonic contents of back-EMF, calculation of desired reference current amplitudes, which are required to eliminate some selected harmonics of torque ripple, are reviewed. In order to inject the reference harmonic currents to the motor windings, an Adaptive Input-Output Feedback Linearization (AIOFBL) control is proposed, which generates the reference voltages for three phases voltage source inverter in stationary reference frame. Experimental results are presented to show the capability and validity of the proposed control method and are compared with the vector control in Multi-Reference Frame (MRF) and Pseudo-Vector Control (P-VC) method results.

© 2017 ISA. Published by Elsevier Ltd. All rights reserved.

1. Introduction

Brushless DC Motors are widely used in many applications such as transport systems and servo drives. Typically, the advantages of these motors, including simple construction, good torque–speed characteristic, high power density, fast dynamic response, high efficiency, long life time and easy to control [1,2].

The major weakness of BLDC motors is the higher torque ripple generation. Some of this ripple is related to the cogging torque which is a result of the effect of the stator slots on the air gap magnetic field and is independent of the stator feeding and can be decreased by skewing the stator slots. The other source of torque ripple is due to the harmonics content of back-emf and can be minimized by feeding the safe stator harmonic current. Therefore, there are two main techniques for torque ripple reduction of BLDCMs: motor structure modification and stator current-shape improvement.

Torque ripple reduction methods based on stator current shaping are such as model reference adaptive control [3], phase current perfectly match to back-EMF [4], lead angle injection in respect to back-emf zero crossing [5–7], current controlled modulation technique [8,9], Pulse Width Modulation (PWM) control [10], direct torque and indirect flux control [11] and also harmonic current injection [12–19]. In [3], an inner control loop is used for shaping of the stator phase currents based on model reference adaptive control. The stator phase current reference is quasi rectangular and the back-EMF shape is trapezoidal. Torque ripple reduction is done by adaptive correction of the stator current slope. If the back-EMF is non-ideal trapezoidal form, the mentioned method cannot be used and should be replaced with adaptive methods to change the amplitude and phase of the harmonic currents which are injected to the stator currents.

Most of the methods for torque ripple reduction using stator current shaping are based on harmonic injection to the stator current. In order to calculate the reference harmonic current amplitudes which are needed to inject to the stator windings, some offline and online techniques have been reported.

In online methods, the stator reference current harmonics are calculated based on some torque ripple minimization algorithms such as repetitive control [12], adaptive self-tuning method based on Fourier coefficients of the generated torque [13], modified vector control [14], cycle average torque control [15] and adaptive decision fusion algorithms [16].

In offline methods, generation of reference currents are performed by constructing a lookup table indexed by position, speed, and required average torque [17–20]. In these methods, the amplitudes of reference current harmonics are precisely calculated to completely eliminate the selected harmonics of torque ripples [18], or by using an optimization method the reference current harmonics are calculated to minimize the torque ripple and even motor losses and maximize the torque per current ratio [19].

In order to inject the calculated harmonic currents to the stator windings, the conventional FOC method cannot be used. Since the harmonic contents of the stator currents in the rotational reference frame will oscillate with 6th multiplies of the fundamental frequency, so the Multi-Reference Frame (MRF) method [20–22] can be used, which is complicated and time consuming method.

Vector control in a MRF is proposed in [20] in order to harmonic injection into the stator windings. In that method, the amplitude of the desired q-axis current, in the each reference frame is assumed as a constant coefficient of the square wave harmonics and the d-axis reference current is set to zero and then the stator current components in the stationary reference frame at each frequency is obtained by Park transformation. Afterwards, the stator reference current components in the stationary reference frame are calculated by the summation of each harmonic current. Then the reference of the stator voltage is calculated by using two PI current controllers. In [21], a MRF synchronous estimator is proposed. The estimation of the stator current harmonic amplitudes using transformation matrices gives a heavy computational burden.

In [22], an adaptive notch filter is used to estimate the stator current harmonics to be implemented in a multi reference frame, and then, by using PI regulators the stator reference voltage components in each reference frame can be derived. After that, by transformation of these reference voltages to the stationary frame and adding them, the stator voltage references are calculated.

So, with the purpose of harmonic current injection in the stator winding, while the machine back-EMF is non-ideal, the control methods which are employed in the stationary reference frame are preferred.

In [23], a Pseudo-Vector Control method is used to generate the reference harmonic currents of BLDC, in which the quadrature component of the stator current is derived using reference torque and the direct component is set to zero. It is obvious that the effects of the higher order of stator currents on the generated torque cannot be considered in that method.

In this paper, a new method based on input-output feedback linearization technique is proposed for injection of harmonic currents to the stator windings in order to reduce electromagnetic torque ripple from a BLDC motor. Since most of the input-output linearization methods are sensitive to model parameters, an adaptive method is proposed to estimate the stator resistance uncertainties. This method can inject the arbitrary reference current to the stator windings using VSI. The stator reference currents are proposed to be calculated based on the elimination of some harmonic contents in the generated torque. Then, by using non sinusoidal reference currents, the proposed method is tested. Finally, in order to evaluate the effectiveness of the proposed method, the results of this method are compared with the multi-reference frame [21,22] and pseudo-vector control [23] methods by experimental tests.

2. Mathematical model of the brushless DC motor

In many reported researches the back-EMF waveform of BLDC is assumed to be sinusoidal [24,25]. However, the actual back-EMF waveform might be quite non-sinusoidal. Including the back-EMF harmonics into the voltage and torque equations increases the accuracy of the model. In [26], eighteen states during an electric angle cycle has been obtained for modeling of non-ideal back-EMF of BLDCM. For small-signal analysis of electromechanical systems the average-value model had been proposed for PMSM with non-sinusoidal back-EMF in [27] and for BLDC with trapezoidal back-EMF in [28].

The equivalent circuit of BLDC motor for each phase is shown in Fig. 1. The electrical dynamics of the BLDC motor is written by the following voltage equations.
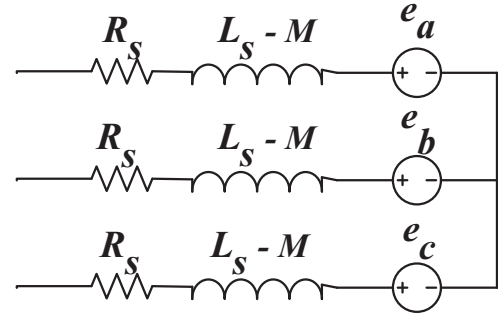
Fig. 1. Equivalent circuit for each motor phase [11].

$$V_{abcs} = r_s i_{abcs} + \frac{d\lambda_{abcs}}{dt} \tag{1}$$

Where the variables are given in vectors such as $f_{abcs} = [f_{as} f_{bs} f_{cs}]^T$, f may refer to the stator voltage respect to the neutral point of the motor winding, current and flux linkage. The stator resistance matrix is as (2).

$$r_s = diag[r_s, r_s, r_s] \tag{2}$$

The flux linkages are then given by

$$\lambda_{abcs} = L_s i_{abcs} + \lambda'_m \tag{3}$$

Where the inductance matrix is defined by

$$L_s = \begin{bmatrix} L_{ls} + L_m & -0.5L_m & -0.5L_m \\ -0.5L_m & L_{ls} + L_m & -0.5L_m \\ -0.5L_m & -0.5L_m & L_{ls} + L_m \end{bmatrix} \tag{4}$$

Where L_{ls} and L_m are the stator leakage and magnetizing inductances, respectively, and λ'_m is the vector of flux linkages.

Assuming that stator windings are wye connected, the sum of the three phase currents equal to zero. Thus, (3) may be simplified as the following.

$$\lambda_{abcs} = L_s i_{abcs} + \lambda'_m \tag{5}$$

Where $L_s = L_{ls} + \frac{3}{2}L_m$.

The comprehensive model considered in this paper has to include the desirable amount of back-EMF harmonics. To contain that, the flux linkage vector can be expressed as the following.

$$\lambda'_m = \lambda'_m \sum_{n=1}^{\infty} K_{2n-1} \begin{bmatrix} \sin\left((2n-1)\theta_r\right) \\ \sin\left((2n-1)\left(\theta_r - \frac{2\pi}{3}\right)\right) \\ \sin\left((2n-1)\left(\theta_r + \frac{2\pi}{3}\right)\right) \end{bmatrix} \tag{6}$$

Where θ_r is the rotor electrical position, and λ'_m is the magnitude of the fundamental component of the permanent magnet flux linkage. The coefficient K_n denotes the normalized magnitude of nth flux harmonic relative to the fundamental, i.e., $K_1 = 1$. Also, the index $2n - 1$ shows that only odd harmonics may be present since the rotor is assumed to be symmetrical.

The developed electromagnetic torque in presence of back-EMF harmonics is then defined as the following [28].

$$T_e = \frac{P}{2}\lambda'_m \sum_{n=1}^{\infty}(2n-1)K_{2n-1}\begin{bmatrix} i_{as} \\ i_{bs} \\ i_{cs} \end{bmatrix}^T \begin{bmatrix} \cos((2n-1)\theta_r) \\ \cos\left((2n-1)\left(\theta_r-\frac{2\pi}{3}\right)\right) \\ \cos\left((2n-1)\left(\theta_r+\frac{2\pi}{3}\right)\right) \end{bmatrix}$$

(7)

The phase back-EMF voltages can be measured at the stator terminals when the machine is rotated by a prime mover and terminals are open circuited. They can be also calculated based on (1)–(6) as follows.

$$e_{abcs} = \omega_r\lambda'_m \sum_{n=1}^{\infty}(2n-1)K_{2n-1}\begin{bmatrix} \cos((2n-1)\theta_r) \\ \cos\left((2n-1)\left(\theta_r-\frac{2\pi}{3}\right)\right) \\ \cos\left((2n-1)\left(\theta_r+\frac{2\pi}{3}\right)\right) \end{bmatrix}$$

(8)

It must be noted that, if the motor back-EMF has triple harmonics, the stator neutral point voltage with respect to the negative dc bus may tolerates with triple harmonics.

The mechanical dynamic equation of motor speed is

$$\frac{d\omega_r}{dt} = \left(\frac{P}{2}\right)\frac{1}{J}(T_e - T_m)$$

(9)

Where ω_r is the rotor electrical angular speed, J is the combined moment of inertia of the load and the rotor, P is the number of magnetic poles, and T_m denotes the combined mechanical torque.

3. Conventional control method based on harmonic injection

3.1. Pseudo-Vector Control (P-VC)

Pseudo Vector Control method in [23] is proposed for torque ripple reduction of BLDC motor with trapezoidal back-EMF. As shown in Fig. 2, the motor back-EMFs are transferred to d-q rotor reference frame, and then the back-EMFs are taking into account in calculation of reference current components in d-q frame by:

$$i_{qs}^* = \frac{\frac{2}{3}T_e^*\omega_m - e_d i_{ds}^*}{e_q}$$

(10)

where i_{qs}^* and i_{ds}^* are the stator reference currents and e_q and e_d are back-EMF components in d-q reference frame. As well as, i_{ds}^* can be selected based on efficiency control method.

The d-q frame is utilized only for calculating these reference currents, while the phase current control principle is normally used in a-b-c frame by conventional PI controller. It is obvious that the back-EMF components in d-q frame are not constant values and are dc superimposed with 6th and higher order harmonics which should be saved in look-up-table.

3.2. Vector control in a Multi Reference Frame (MRF)

In vector control with Multi reference frame, the stator current variable is transferred to multi reference frame which rotates with $k\omega_r$ by transformation matrix (11).

$$K^x = \frac{2}{3}\begin{bmatrix} \cos(x\theta_r) & \cos\left(x\left(\theta_r-\frac{2\pi}{3}\right)\right) & \cos\left(x\left(\theta_r+\frac{2\pi}{3}\right)\right) \\ \sin(x\theta_r) & \sin\left(x\left(\theta_r-\frac{2\pi}{3}\right)\right) & \sin\left(x\left(\theta_r+\frac{2\pi}{3}\right)\right) \\ \frac{1}{2} & \frac{1}{2} & \frac{1}{2} \end{bmatrix}$$

(11)

As shown in Fig. 3, in order to obtain the stator current components in each reference frame, low pass filters are used. The reference voltage components in each frame can be produced using conventional PI controllers. After that, the reference voltage which rotates with $k\omega_r$, can be calculated by the inverse transformation of K^x. Finally the stator reference voltage can be calculated by adding all previous generated voltages in each reference frame.

4. Input Output Feedback Linearization Controller Design (IOFBL)

Substituting (3) in (1), the electrical dynamics of BLDC motor
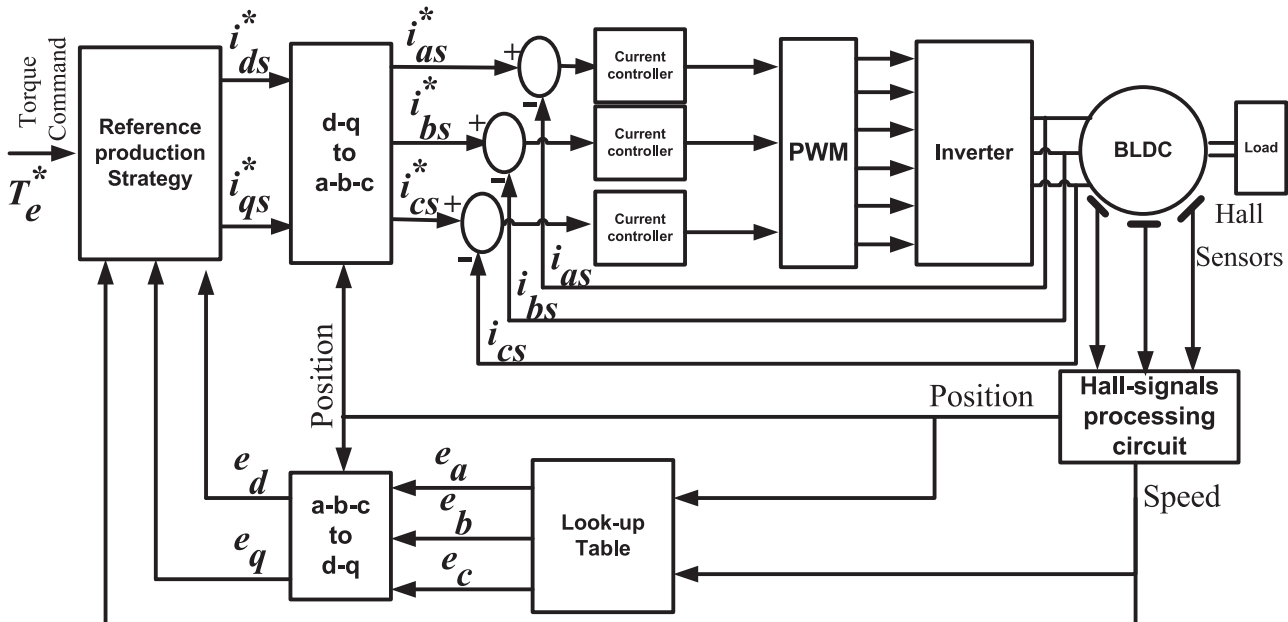
Fig. 2. Block-diagram of the Pseudo-Vector Control.
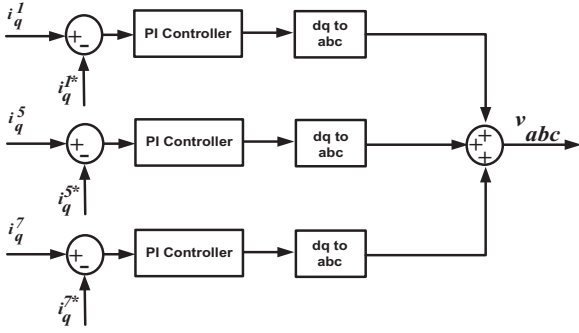
Fig. 3. Multiple Reference Frame Controller.

function of phase currents, can be written as (10).

$$\boldsymbol{V}_{abcs} = \boldsymbol{r}_s\boldsymbol{i}_{abcs} + L_s\frac{d\boldsymbol{i}_{abcs}}{dt} + \frac{d\lambda'_m}{dt} \tag{12}$$

then this is described as (13).

$$\frac{d\boldsymbol{i}_{abcs}}{dt} = \frac{1}{L_s}\left(\boldsymbol{V}_{abcs} - \boldsymbol{r}_s\boldsymbol{i}_{abcs} - \frac{d\lambda'_m}{dt}\right) \tag{13}$$

If the $\boldsymbol{i}^*_{abcs} = \left[\,\boldsymbol{i}^*_{as}\boldsymbol{i}^*_{bs}\boldsymbol{i}^*_{cs}\,\right]^T$ is the currents reference vector, the error dynamics system can be written as (14).

$$\frac{d\boldsymbol{i}_{abcs}}{dt} - \frac{d\boldsymbol{i}^*_{abcs}}{dt} = \frac{1}{L_s}\left(\boldsymbol{V}_{abcs} - \boldsymbol{r}_s\boldsymbol{i}_{abcs} - \frac{d\lambda'_m}{dt}\right) - \frac{d\boldsymbol{i}^*_{abcs}}{dt} \tag{14}$$

Defining the currents error vector as $\boldsymbol{e}_{abcs} = \boldsymbol{i}_{abcs} - \boldsymbol{i}^*_{abcs}$, the error dynamics is expressed as (15).

$$\frac{d\boldsymbol{e}_{abcs}}{dt} = \frac{1}{L_s}\left(\boldsymbol{V}_{abcs} - \boldsymbol{r}_s\boldsymbol{i}_{abcs} - \frac{d\lambda'_m}{dt}\right) - \frac{d\boldsymbol{i}^*_{abcs}}{dt} \tag{15}$$

Based on the IOFBL method, the control laws of this system, $\boldsymbol{V}_{abcs}$, can be defined as (16).

$$\boldsymbol{V}_{abcs} = \boldsymbol{r}_s\boldsymbol{i}_{abcs} + L_s\frac{d\boldsymbol{i}^*_{abcs}}{dt} + \frac{d\lambda'_m}{dt} - KL_s\boldsymbol{e}_{abcs} \tag{16}$$

where K is positive Lyapunov constant. Substituting (16) in (15), the error dynamics equations of BLDC motor is produced as (17).

$$\frac{d\boldsymbol{e}_{abcs}}{dt} = -K\boldsymbol{e}_{abcs} \tag{17}$$

Since K is positive constant, therefore the currents error vector, $\boldsymbol{e}_{abcs}$, converge exponentially to zero. This means that $\boldsymbol{i}_{abcs}$ will converge to their desired reference, $\boldsymbol{i}^*_{abcs}$.

4.1. Adaptive Input Output Feedback Linearization (AIOFBL)

Since the stator resistance value is not accurately known and varies with the motor temperature, it is required to estimate this parameter. Suppose that the stator resistance is uncertain and $\hat{R}_s$ is its estimation, therefore the control inputs can be written as the following

$$\boldsymbol{V}_{abcs} = \hat{\boldsymbol{r}}_s\boldsymbol{i}_{abcs} + L_s\frac{d\boldsymbol{i}^*_{abcs}}{dt} + \frac{d\lambda'_m}{dt} - KL_s\boldsymbol{e}_{abcs} \tag{18}$$

where $\hat{\boldsymbol{r}}_s = \text{diag}\left[\,\hat{r}_s, \hat{r}_s, \hat{r}_s\,\right]$. Substituting (18) in (15), the error dynamics equations of BLDC motor is produced as (19).

$$\frac{d\boldsymbol{e}_{abcs}}{dt} = \frac{1}{L_s}\left(\left(\hat{\boldsymbol{r}}_s - \boldsymbol{r}_s\right)\boldsymbol{i}_{abcs}\right) - K\boldsymbol{e}_{abcs} \tag{19}$$

In order to show the stability of the controller and obtain the adaptation law for the stator resistance, a positive definite

Lyapunov function is selected as (20).

$$V = \frac{1}{2}\boldsymbol{e}^T_{abcs}\boldsymbol{e}_{abcs} + \frac{1}{2\eta}\left(\hat{\boldsymbol{r}}_s - \boldsymbol{r}_s\right)^2 > 0 \tag{20}$$

where η is a positive tuning parameter. The time derivative of Lyapunov function can be written as (21).

$$\dot{\boldsymbol{V}} = \boldsymbol{e}^T_{abcs}\dot{\boldsymbol{e}}_{abcs} + \frac{1}{\eta}\hat{\boldsymbol{r}}_s\left(\hat{\boldsymbol{r}}_s - \boldsymbol{r}_s\right) = \boldsymbol{e}^T_{abcs}\left(\frac{1}{L_s}\left(\left(\hat{\boldsymbol{r}}_s - \boldsymbol{r}_s\right)\boldsymbol{i}_{abcs}\right) - K\boldsymbol{e}_{abcs}\right)$$

$$+ \frac{1}{\eta}\hat{\boldsymbol{r}}_s\left(\hat{\boldsymbol{r}}_s - \boldsymbol{r}_s\right) = -K\boldsymbol{e}^T_{abcs}\boldsymbol{e}_{abcs} + \left(\hat{\boldsymbol{r}}_s - \boldsymbol{r}_s\right)\left(\frac{1}{L_s}\left(\boldsymbol{e}^T_{abcs}\boldsymbol{i}_{abcs}\right) + \frac{1}{\eta}\hat{\boldsymbol{r}}_s\right) \tag{21}$$

where $\hat{\boldsymbol{r}}_s = \text{diag}\left[\,\hat{r}_s, \hat{r}_s, \hat{r}_s\,\right]$. If the second term of (21) forced to zero as (22).

$$\left(\hat{\boldsymbol{r}}_s - \boldsymbol{r}_s\right)\left(\frac{1}{L_s}\left(\boldsymbol{e}^T_{abcs}\boldsymbol{i}_{abcs}\right) + \frac{1}{\eta}\hat{\boldsymbol{r}}_s\right) = 0 \tag{22}$$

The estimation mechanism is produced from (22) as the following.

$$\hat{\boldsymbol{r}}_s = -\frac{\eta}{L_s}\left(\boldsymbol{e}^T_{abcs}\boldsymbol{i}_{abcs}\right) \tag{23}$$

So, the derivative of Lyapunov function, $\dot{\boldsymbol{V}}$, will be negative semi-definite as (24).

$$\dot{\boldsymbol{V}} = -K\boldsymbol{e}^T_{abcs}\boldsymbol{e}_{abcs} \tag{24}$$

Therefore, the system is shown in (19) and (23) is stable. If the Lyapunov function (20) is bounded, then the error system is bounded too and therefore $\dot{\boldsymbol{V}}$ is uniformly continuous, because its derivative is bounded as following,

$$\ddot{\boldsymbol{V}} = -2K\boldsymbol{e}^T_{abcs}\dot{\boldsymbol{e}}_{abcs} < \infty \tag{25}$$

Finally, using Barbalat's Lemma, the derivative of Lyapunov function (24), goes to zero and then errors E_α and E_β will converge asymptotically to zero [29].

5. Selected Torque Harmonic Elimination Method (STHE)

If the back-EMF harmonic contents are known, by injection of some specific harmonic currents in the stator windings, some of the torque harmonics can be eliminated. So, based on offline method proposed in [18], the amplitude of the stator currents harmonics can be obtained.

If the stator currents have the same harmonic contents of the back-EMF, except the third harmonics order, and also the phase differences between the currents and back-EMFs is zero, the stator currents can be written as:

$$\mathrm{I}_{abcs} = \sum_{m=0}^{\infty}\left(I_{6m+1}\begin{bmatrix} \cos\left((6m+1)\theta_r\right) \\ \cos\left((6m+1)\left(\theta_r - \frac{2\pi}{3}\right)\right) \\ \cos\left((6m+1)\left(\theta_r + \frac{2\pi}{3}\right)\right) \end{bmatrix}\right)$$

$$+ \sum_{m=1}^{\infty}\left(I_{6m-1}\begin{bmatrix} \cos\left((6m-1)\theta_r\right) \\ \cos\left((6m-1)\left(\theta_r - \frac{2\pi}{3}\right)\right) \\ \cos\left((6m-1)\left(\theta_r + \frac{2\pi}{3}\right)\right) \end{bmatrix}\right) \tag{26}$$

It is important to note that the stator current harmonics of order multiple three are not considered because of Y connection of
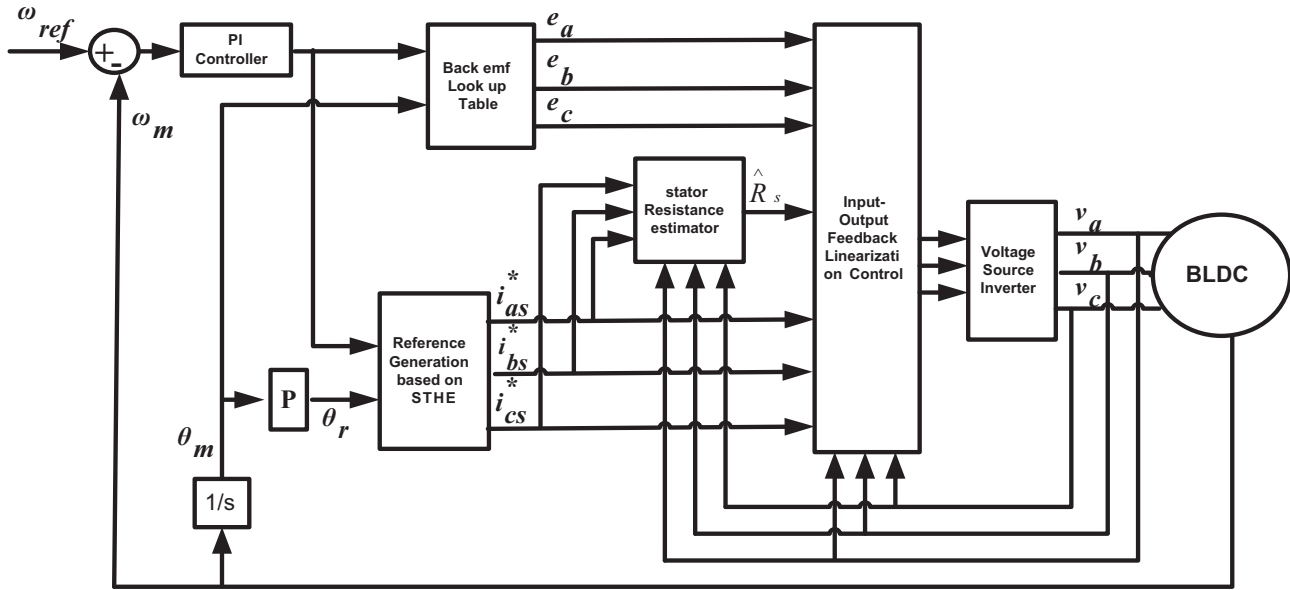
Fig. 4. Block diagram of the proposed method based on AIOFBL.

motor windings as well as extra torque ripple of third harmonic current. By replacing (26) in (7), the following equation is obtained for motor torque.

$$T_e = \frac{P}{2}\lambda'_m \left(\sum_{m=1}^{\infty} \sum_{n=1}^{\infty} \left((2n-1)I_{6m-1}K_{2n-1} \begin{bmatrix} \cos((6m-1)\theta_r) \\ \cos\left((6m-1)\left(\theta_r-\frac{2\pi}{3}\right)\right) \\ \cos\left((6m-1)\left(\theta_r+\frac{2\pi}{3}\right)\right) \end{bmatrix}^T \begin{bmatrix} \cos((2n-1)\theta_r) \\ \cos\left((2n-1)\left(\theta_r-\frac{2\pi}{3}\right)\right) \\ \cos\left((2n-1)\left(\theta_r+\frac{2\pi}{3}\right)\right) \end{bmatrix} \right) \right.$$
$$\left. + \sum_{m=0}^{\infty} \sum_{n=1}^{\infty} \left((2n-1)I_{6m+1}K_{2n-1} \begin{bmatrix} \cos((6m+1)\theta_r) \\ \cos\left((6m+1)\left(\theta_r-\frac{2\pi}{3}\right)\right) \\ \cos\left((6m+1)\left(\theta_r+\frac{2\pi}{3}\right)\right) \end{bmatrix}^T \begin{bmatrix} \cos((2n-1)\theta_r) \\ \cos\left((2n-1)\left(\theta_r-\frac{2\pi}{3}\right)\right) \\ \cos\left((2n-1)\left(\theta_r+\frac{2\pi}{3}\right)\right) \end{bmatrix} \right) \right) \tag{27}$$

So, the torque profile can be written as (28).

$$T = T_0 + T_6\cos 6\theta_r + T_{12}\cos 12\theta_r + \dots \tag{28}$$

where

$$T_0 = \frac{3P\lambda'_m}{2}\left(K_I I_1 + \sum_{m=1}^{\infty}\left((6m-1)K_{6m-1}I_{6m-1} + (6m+1)K_{6m+1}I_{6m+1}\right)\right) \tag{29}$$

$$T_6 = \frac{3P\lambda'_m}{2}\left((7K_7 I_1 + K_I I_7) - (5K_5 I_1 + K_I I_5)\right.$$
$$\left. + \sum_{m=1}^{\infty}\left((6m-1)K_{6m-1}I_{6m+5} + (6m+1)K_{6m+1}I_{6m+7}\right)\right) \tag{30}$$

$$T_{12} = \frac{3P\lambda'_m}{2}\left((K_I I_{13}+13K_{13}I_1) - (K_I I_{11} + 11K_{11}I_1) - (5K_5 I_7+7K_7 I_5)\right.$$
$$\left. + \sum_{m=1}^{\infty}\left((6m-1)K_{6m-1}I_{6m+11} + (6m+1)K_{6m+1}I_{6m+13}\right)\right) \tag{31}$$

In general, the most important torque harmonics are T_6 and T_{12} which are functions of low-order harmonics of the back-EMF and the stator currents.

If the harmonic order of the stator current increased, the effective resistance of the motor windings will be increased, so the copper loss will be increased. As well as, in higher harmonic order

of the stator current the iron loss will be enlarged. So, by assuming the stator harmonic currents higher than 7th order to be zero, the problem will be summarized as the following.

$$\begin{bmatrix} K_1 & 5K_5 & 7K_7 \\ 7K_7-5K_5 & -K_1 & K_1 \\ 0 & 7K_7 & 5K_5 \end{bmatrix} \times \begin{bmatrix} I_1 \\ I_5 \\ I_7 \end{bmatrix} = \frac{2}{3}\begin{bmatrix} T_0 \\ 0 \\ 0 \end{bmatrix} \tag{32}$$

where T_0 is the average demanded torque.

Calculation of (32) may be time-consuming and highly dependent to back-EMF harmonic contents of motor. So, for simplicity, if the amplitude of the harmonic currents is selected such as

$$\frac{I_5}{I_7} = \frac{7K_7}{5K_5} \tag{33}$$

The amplitude of generated torque harmonics will be obtained as:

$$T_0 = \frac{3}{2}\left[K_I I_1 + 10K_5 I_5\right] \tag{34}$$

$$T_6 = 0 \tag{35}$$

Table 1
Nominal BLDC motor parameters.

Parameters	Amount
Number of pole pairs: P	2
Moment of inertia: J	0.0003 Nms^2
Stator resistance: R_s	0.15??
Equivalent inductance of phase windings: $L_s - M$	0. 25 mH
Speed: N	2500 Rpm
Stator current: Is	3.5 A
DC voltage: V_{DC}	90 V
Back-EMF constant	0.026 v/rad/s

Table 2
Nonlinear controller parameters.

Parameters	Amount
Lyapunov constant k	1
Tuning parameter η	3

$$T_{12} = -21K_7I_5 \qquad (36)$$

So, the average generated torque will be greater than sinusoidal stator current and T_6 will be zero and T_{12} is so small that can be negligible.

6. Results

6.1. Experimental setup

Block diagram of the proposed control method is shown in Fig. 4. As shown in this Figure, the input-output feedback linearization method is used to generate the arbitrary reference currents for the stator windings by calculation of the required reference voltage for VSI. This structure has an external loop for speed control and generates the amplitude of the stator reference currents. The parameters of BLDC motor and nonlinear controller are listed in Tables 1 and 2 respectively.

Reference production block calculates the amplitude of the reference stator current harmonics, which should be injected to the stator windings, as shown in Fig. 4. It should be emphasized that, in order to minimize the motor losses and maximize the torque per ampere ratio, each phase stator current's reference should be in-phase with the corresponding phase back-EMF [4]. As well as, by multiplying a constant coefficient in the amplitude of the stator current harmonics, the motor average torque can be controlled. Therefore, one of the inputs of this block is the magnitude of this coefficient, which can be obtained from a PI speed controller, and the other input is the rotor position.

For experimental evaluation of the actual system, a DSP-based prototype is built and tested. The practical setup regarding overall

(a)

(b)

(c)
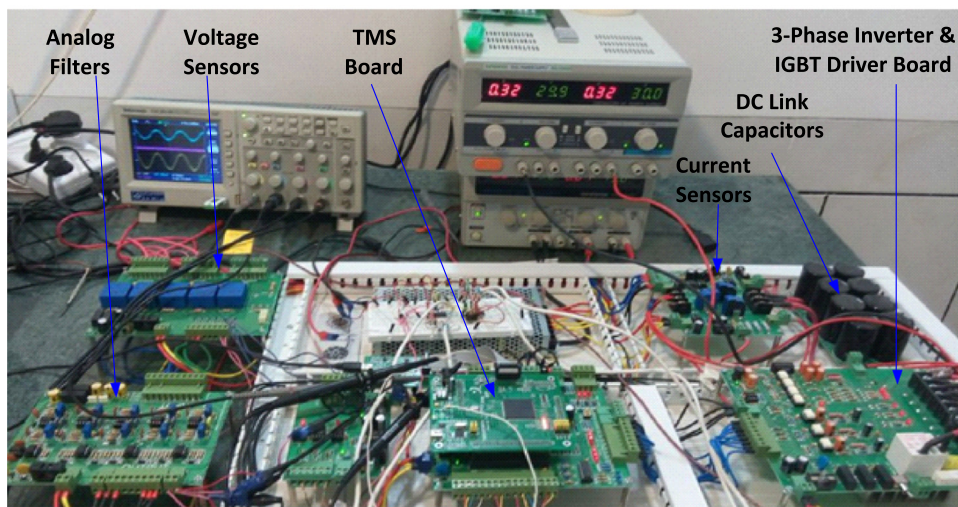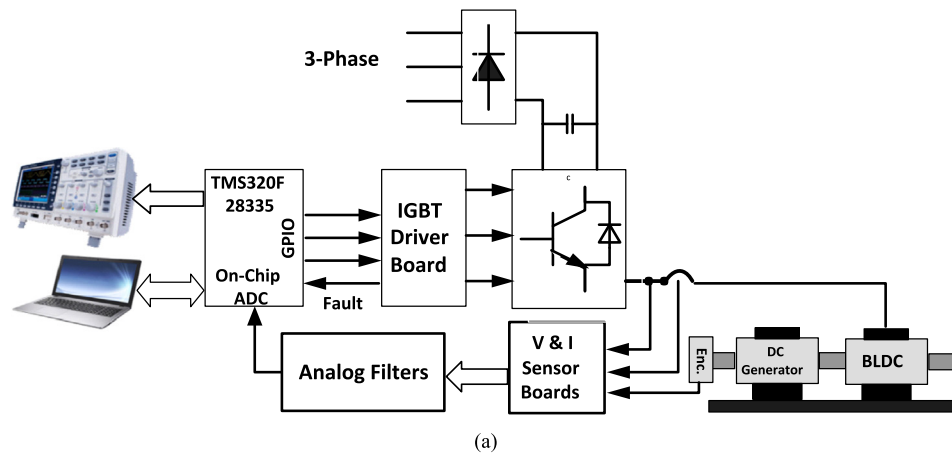
Fig. 5. a) Block diagram of experimental setup of the BLDC motor drive system b) Experimental setup of the BLDC motor drive system c) BLDC motor connected to DC generator as a load torque.
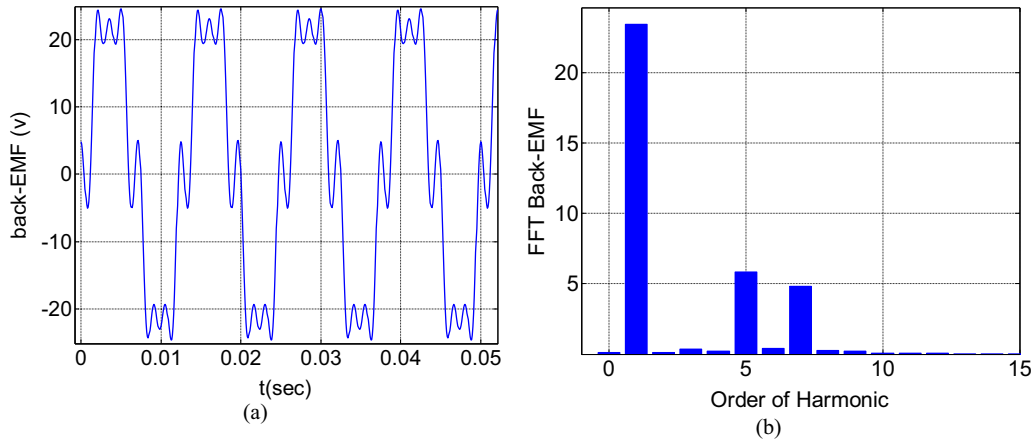
Fig. 6. a) Phase to phase back-EMF profile of the BLDC motor in 2400 Rpm b) FFT of the phase 'a' back- EMF.

Table 3
The harmonic contents of motor back-EMF.

Harmonic order	Per unit amount
1	1
5	−0.25
7	−0.236

Table 4
DC Generator specifications.

Characteristic	Amount
Power	250 W
Voltage	24 VDC
Nominal current	13.5 A
Rated speed	2750 Rpm

Fig. 7. Experimental results: Four quadrant operation of BLDC with P-VC method, a) Motor torque (N.m), b) Motor mechanical speed (rad/sec) c) Motor reference speed (rad/sec).

system block diagram shown in Fig. 5 consists of the following sections: a 300 W BLDC motor with non-sinusoidal back-EMF, voltage source inverter and its driver board, sensor board and a TMS320F28335 discrete signal processor board.

A 250 W DC generator with an external rheostat in the armature terminal is used as a generator load. The DC generator specifications are listed in Table 4.

Rotor position is detected by means of an incremental encoder with 1024 pulses per round mounted on the DC generator shaft.

TMS320F28335 microcontroller designed with Texas Instrument Co. for motor control application with floating point computation capability, 68 KB RAM and 512 KB ROM inside it.

To measure the stator phase currents, two Hall-effect current sensors (LEM LTS-6-NP) are used and the line-to-line voltage is measured by voltage sensors (LEM LV-25-P). All measured stator current and voltage signals are filtered by analog second-order low pass filters with cut-off frequency of about 2.6 kHz and convert to digital by 10-bit on-chip A/D converter with 500 ns conversion time.

The inverter has been designed using low loss IGBT module SKM40GD124D (with 40 A, 1200 V ratings) and intelligent IGBT drivers, HCPL 316 J, which guarantee electrical isolation between the power and the control systems. The inverter switching frequency is 10 kHz and a dead-time equal to 1 μsec is used for shoot-through protection of inverter switches.

The experimental setup is completely modular and each of the mentioned boards is supplied with a 24 v dc power supply and the requested voltage levels are constructed with switching MINMAX regulators. As well as, in order to show the calculated variables in the DSP on the oscilloscope, DAC-PWM output of DSP can be used which can convert the PWM value of the mentioned variable to an analog data via a low pass filter. For example the motor reference speed and its measured values, can be changed to PWM pulses inside the DSP and converted to analog variables and depicted on an oscilloscope.

6.2. Experimental results

Experiments are performed to evaluate the effects of the proposed control method and some conventional offline harmonic injection methods on the torque ripple of a BLDC motor.

The phase to phase back-EMF profile of the BLDC motor in 2400 Rpm is depicted in Fig. 6-a and its FFT profile is shown in Fig. 6-b. The harmonic contents of the motor back-EMF are listed in Table 3.

In Figs. (7–9) the behavior of the BLDC motor in 4-quadrant operation is evaluated based on three different methods i)MRF,
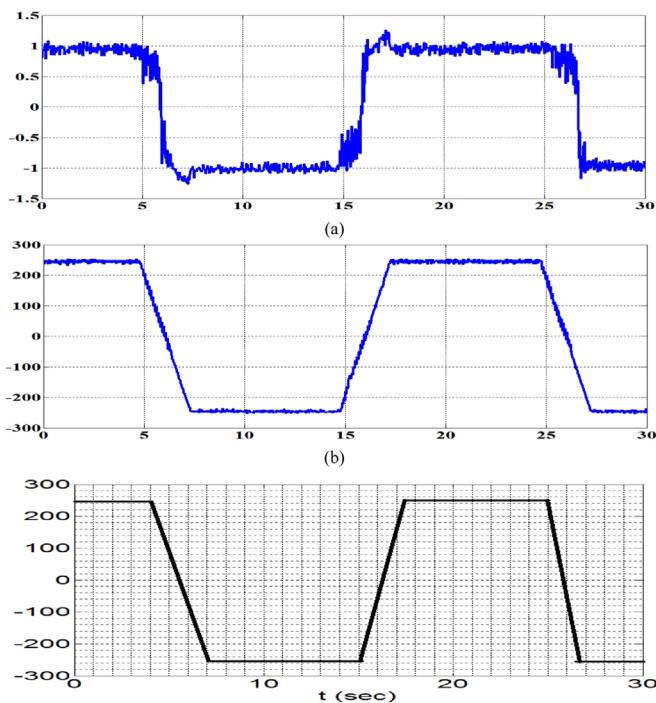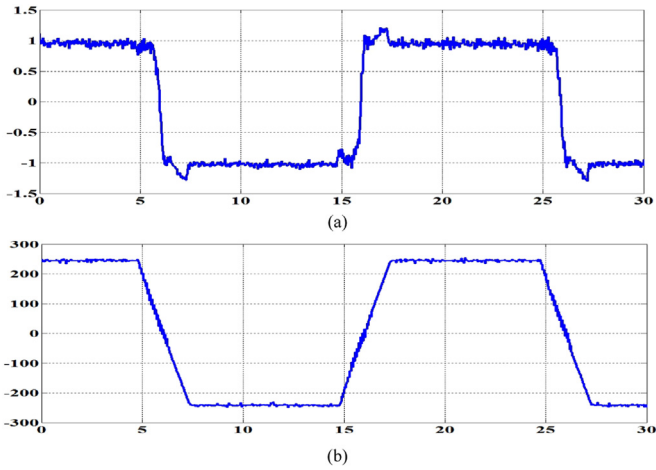
Fig. 8. Experimental results: Four quadrant operation of BLDC with MRF method a) Motor torque (N.m), b) Motor mechanical speed (rad/sec).
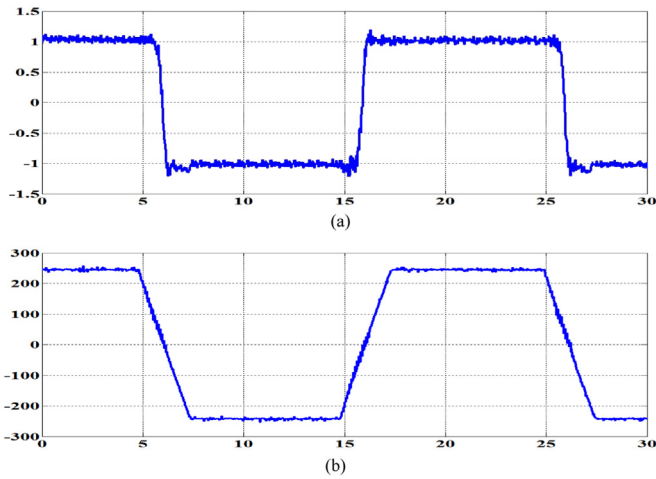
Fig. 9. Experimental results: Four quadrant operation of BLDC with AIOFBL method a) Motor torque (N.m), b) Motor mechanical speed (rad/sec).
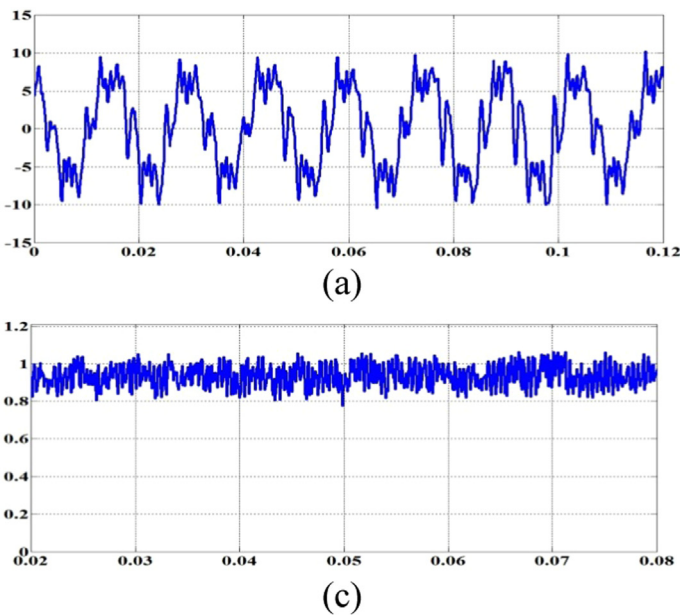
which is mentioned in [227] ii) P-VC, which is reported in [23] and iii) AIOFBL with STHE, respectively. In these tests the transient as well as steady state behavior of the motor is tested. The motor speed reference is a trapezoidal form with amplitude of 250 rad/sec in forward and reverse operation region and its direction is changed with 200 rad/sec per sec. the reference speed is identical for all three control methods. As can be seen, the motor speed tracks the reference waveform in each three methods.

In order to detailed comparison of this methods effects on the generated torque ripple, the steady state operation of these methods are analyzed in Figs. (10–12). As can be seen, the FFT of the stator currents and generated torques are presented in part (a) and (b) of the mentioned figures, respectively. If the THD of the stator current and Ripple Factor of generated torque are calculated as:

$$THD_i = \frac{\sqrt{I_5^2 + I_7^2 + I_{11}^2 + I_{13}^2}}{I_1} \qquad (37)$$

$$RF_T = \frac{\sqrt{\sum_{k=1}^{7} T_{2k}^2}}{T_0} \qquad (38)$$

THD_i and RF_T are calculated and listed in Table 5. As can be seen, the RF_T index in AIOFBL is less than MRF and P-VC methods. As well as, the THD_i of the proposed method is a little better than MRF and significantly better than P-VC methods.

In Fig. 13, the profile of back-EMF phase "a" and its stator current are depicted. As can be seen, the stator current i_a is relatively in-phase with back-EMF, e_a in AIOFBL method. As mentioned in [4], if the phase difference between the back-EMF and stator current is zero, the ratio of average Torque per Ampere (T/I) will be increased. As can be seen in Table 5, the (T/I) of the proposed method is slightly better than the other methods.

Generally, input-output feedback linearization methods are sensitive to model parameters. So, adaptive techniques are used to estimate the model parameters that may be changed with temperature, saturation and so on. In the last test, the robustness of the proposed method against the stator resistance uncertainties is examined. So an initial error for the stator resistance is assumed in the controller block (R_s is assumed to be 0.45?? at t=2 s while its true value is 0.15??). The results of this scenario are shown in

Fig. 10. Experimental results: P-VC method. a) i_a (A) b) Motor torque T_e (N.m) c) FFT of motor phase current d) FFT of motor torque.
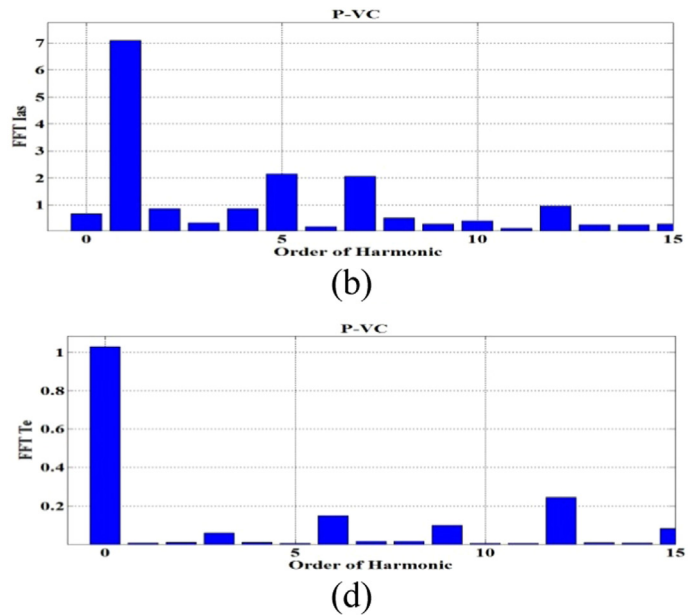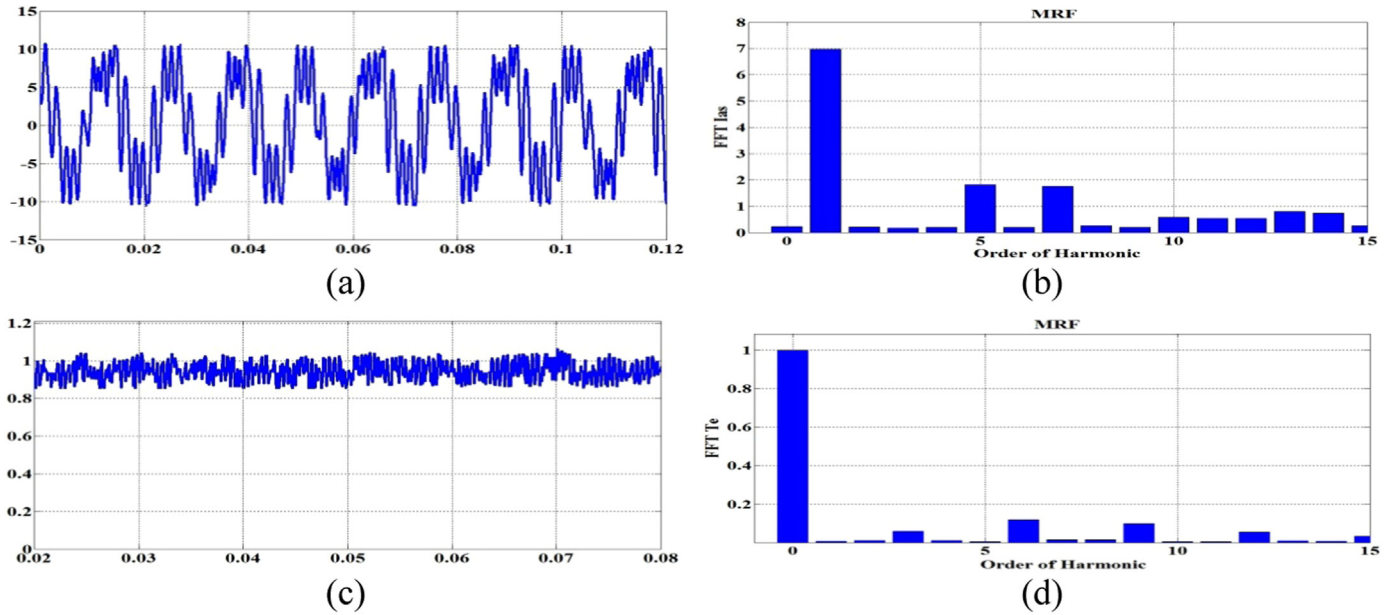
Fig. 11. Experimental results: MRF method a) i_a (A) b) Motor torque T_e (N.m) c) FFT of motor phase current d) FFT of motor torque.
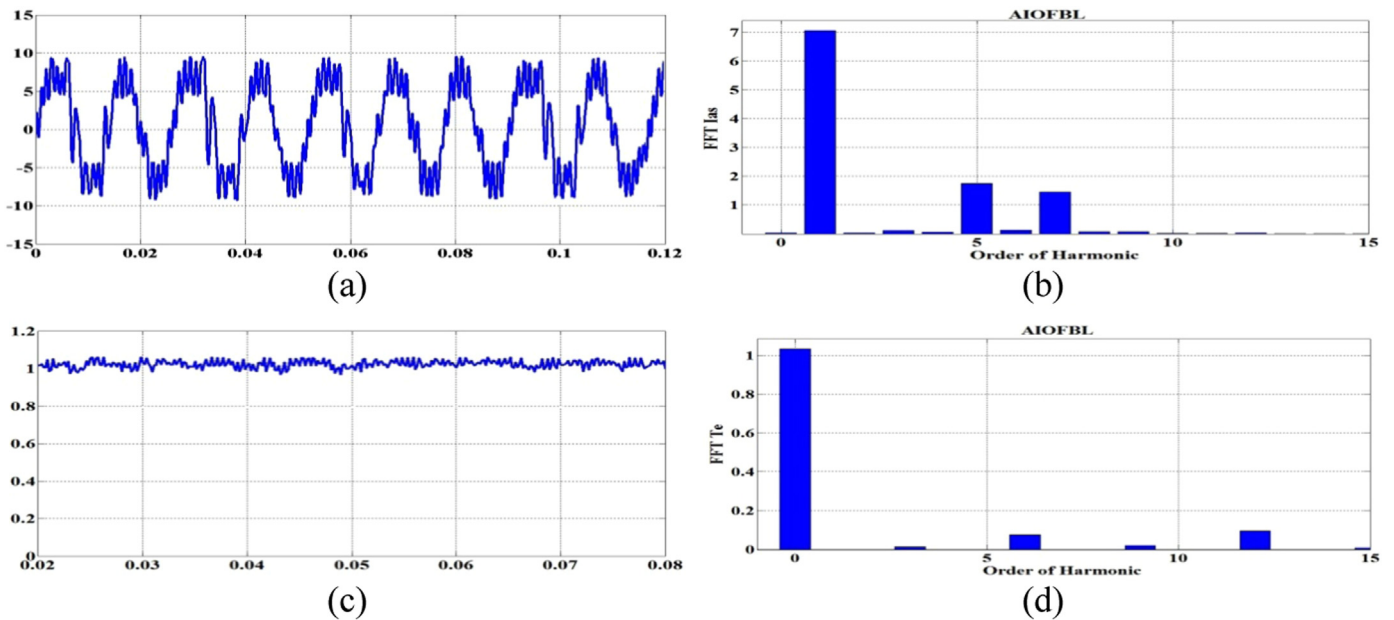
Fig. 12. Experimental results: AIOFBL a) i_a (A) b) Motor torque T_e (N.m) c) FFT of motor phase current d) FFT of motor torque.

Table 5
THD of the stator current and Ripple Factor of the generated torque and T/I ratio.

	P-VC	MRF	AIOFBL
THD$_i$	0.423	0.371	0.323
RF$_T$	0.278	0.130	0.110
T/I	0.145	0.144	0.146

Fig. 14, where the motor speed (cyan), the motor torque (yellow) and R_s variation (pink) are shown. In order to show the motor speed, its reference and the stator resistance values, which is set inside the digital controller, on the oscilloscope, the PWM-DAC output of the TMSF28335 is used.

It must be noted the proposed AIOFBL method is realized in stationary reference frame and in contrast to the P-VC and MRF, no needs to additional filter to select the harmonic contents of the stator currents in each reference frame like as MRF and P-VC methods.

7. Conclusions

The aim of this paper is to develop a control technique for torque ripple reduction in brushless DC motor. STHE is used to select the proper reference harmonic current for injection to the stator windings. In order to inject the desired harmonic currents to the stator windings, the conventional vector control in the
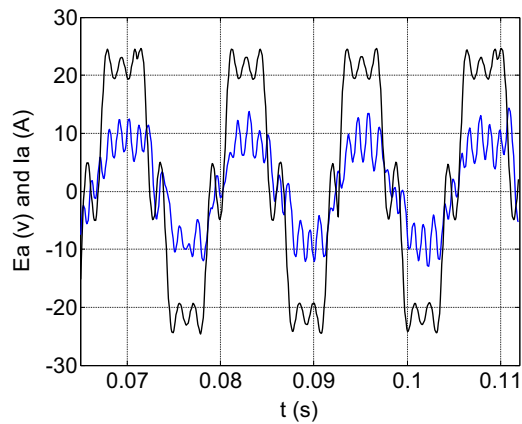
Fig. 13. Experimental results: Back-EMF and stator current with AIOFBL.
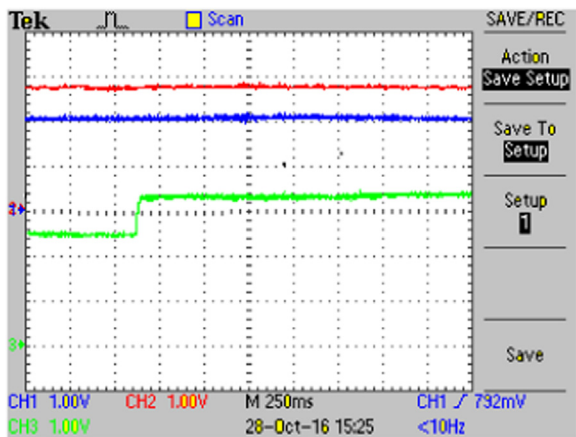
Fig. 14. Experimental results: AIOFBL method robustness against R_s variation (BLDC motor Speed: cyan, BLDC motor Torque (0.3 Nm/div): yellow, R_s variation: pink).

synchronous reference frame cannot be applicable. Then an adaptive input-output feedback linearization method is proposed to generate the stator reference voltages in the stationary reference frame. This method no needs to any extra filter to obtain the amplitude of each harmonic order in the stator current. The effectiveness of the proposed method is evaluated by experimental tests and is compared with P-VC and MRF methods.

Acknowledgement

References

[1] Hendershort Jrand JR, Miller THE. Design of brushless permanent-magnet machines.Venice, FL: Motor Design Books; 2010.
[2] Low TS, Tseng KJ, Lee TH, Lim KW, Lock KS. Strategy for the instantaneous torque control of permanent-magnet brushless DC drives. IEE Proceedings B (Electric Power Applications), 137-6; 1990, p. 355–363.
[3] Sozer Y, and Torrey DA. Adaptive torque ripple control of permanent magnet brushless DC motors. Applied Power Electronics Conference and Exposition (APEC '98). Vol. 1; 1998, p. 86–92.
[4] Park SJ, Park HW, Lee MH, Harashima F. A new approach for minimum-torque-ripple maximum-efficiency control of BLDC motor. IEEE Trans Ind Appl :2000;47-1:109–14.
[5] Im WS, Kim JP, Kim JM, Baek KR. Torque maximization control of 3-phase BLDC motors in the high speed region. J Power Electron : 2010;10-6:713–23.
[6] Lee SJ, Hong JP, Jang WK. Characteristics comparison of BLDC motor according to the lead angles. VPPC 2012;2012:879–83.
[7] Gu BG, Choi JH, Jung IS. Simple lead angle adjustment method for brushless DC motors. J Power Electron 2014;14-3:541–8.
[8] Karthikeyan J, Sekaran RD. Current control of brushless dc motor based on a common dc signal for space operated vehicles. Electr Power Energy Syst 2011;33:1721–7.
[9] Carlson R, Lajoie-Mazenc M, Fagundes JCDS. Analysis of torque ripple due to phase commutation in brushless DC machines. IEEE Trans Ind Appl 2002;28-3:632–8.
[10] Krishnan G, Ajmal KT. A Neoteric Method Based on PWM ON PWM Scheme with Buck Converter for Torque Ripple Minimization in BLDC Drive. International Conference on Magnetics, Machines & Drives (AICERA-2014 iCMMD); 2014.
[11] Ozturk SB, Alexander WC, Toliyat HA. Direct torque control of four-switch brushless DC motor with non-sinusoidal backEMF. IEEE Trans Power Electron 2010;25-2:263–71.
[12] Mattavelli P, Tubiana L, Zigliotto M. Torque-ripple reduction in PM synchronous motor drives using repetitive current control. IEEE Trans Power Electron 2005;20-6:1423–31.
[13] Aghili F. Adaptive reshaping of excitation currents for accurate torque control of brushless motors. IEEE Trans Control Syst Technol 2008;16-2:356–64.
[14] Kshirsagar P, Krishnan R. High-efficiency current excitation strategy for variable-speed nonsinusoidal Back-EMF PMSM machines. IEEE Trans Ind Appl 2012;48-6:1875–89.
[15] Sheng T, Wang X, Zhang J, Deng Z. Torque-ripple mitigation for brushless DC machine drive system using one-cycle average torque control. IEEE Trans Ind Electron 2015;62:2114–22.
[16] Erken F, Öksüztepe E, Kürüm H. Online adaptive decision fusion based torque ripple reduction in permanent magnet synchronous motor. March: 2016. 10-3, p. 189–196.
[17] Hung JY, Ding Z Minimization of Torque Ripple in Permanent Magnet Motors: A Closed Form Solution. International Conference on Industrial Electronics, Control, Instrumentation, and Automation; 1992. 1. p. 459–463.
[18] Hanselman DC. Minimum torque ripple, maximum efficiency excitation of brushless permanent magnet motors. IEEE Trans Ind Appl 1994;41:292–300.
[19] LeHuy H, Perret R, Feuillet R. Minimization of torque ripple in brushless DC motor drive. IEEE Trans Ind Appl 1986;22:748–55.
[20] Kim TS, Ahn SC, and Hyun DS. A New Current Control Algorithm for Torque Ripple Reduction of BLDC Motors, In: Industrial Electronics Society. IECON '01. In: Proceedings of the 27th Annual Conference of the IEEE; 2001, p. 1521–1526.
[21] Chapman PL, Sudhoff SD. A multiple reference frame synchronous estimator/regulator. IEEE Trans Energy Convers 2000;15(2):197–202.
[22] Amirian MA, Rashidiand A, and Nejad SMSaghaeian. Torque ripple reduction of permanent magnet synchronous motor with non-sinusoidal back-EMF using a modified and simplified current optimization technique, In: Proceedings 6th Power Electronics, Drive Systems & Technologies Conference PEDSTC; 2015, p. 322–327.
[23] Ta CM. Pseudo-vector Control – An Alternative Approach for Brushless DC Motor Drives. IEEE, IEMDC 2011, p. 1534-1539.
[24] Sudhoff SD, Krause PC. Operation modes of the brushless DC motor with a 120∞inverter. IEEE Trans Energy Convers 1990;5(3):558–64.
[25] Han Q, Samoylenko N. Average-value modeling of brushless DC motors with 120∞voltage source inverter. IEEE Trans Energy Convers . 2008;23(2):423–32.
[26] Zhao Y, Yang YJ. Modeling and simulation of brushless DC motor with non-ideal back-EMF. Appl Mech Mater 2012;130–134:3434–7.
[27] Chapman PL, Sudhoff SD, Whitcomb CA. Multiple reference frame analysis of non-sinusoidal brushless DC drives. IEEE Trans Energy Conv . 1999;14(3):440–6.
[28] Tabarraee K, Iyer J, Atighechi H, Jatskevich J. Dynamic average-value modeling of 120° VSI commutated brushless dc motors with trapezoidal back-EMF. IEEE Trans Energy Convers 2012;27:296–307.
[29] Slotine JJE, Li W. Applied nonlinear control. Prentice-Hall, Inc; 1991.